

## Presence of tri-iodide ions in iodine-intercalated $\text{IBi}_2\text{Sr}_2\text{CaCu}_2\text{O}_8$ superconductors

Pham V. Huong and A. L. Verma\*

Laboratoire de Spectroscopie Moléculaire et Cristalline, Université Bordeaux I, 351, Cours de la Libération, 33405 Talence, France

(Received 29 March 1993)

Stage-1 iodine-intercalated  $\text{IBi}_2\text{Sr}_2\text{CaCu}_2\text{O}_8$  single crystals with  $T_c = 78$  K were studied by Raman microspectroscopy in comparison with undoped  $\text{Bi}_2\text{Sr}_2\text{CaCu}_2\text{O}_8$ . Evidence is shown for the existence of an asymmetrical  $I_3^-$  state and a weak interaction is revealed between this ion and the adjacent Bi-O layers. The phonon coupling that initially exists in the identical, close, and staggered Bi-O bonds along the  $c$  axis, disappears as a result of the iodine intercalation in the host network where the Bi-O bonds become aligned along this  $c$  axis.

### I. INTRODUCTION

The microstructure and properties of the  $\text{Bi}_2\text{Sr}_2\text{CaCu}_2\text{O}_8$  (Bi 2:2:1:2) superconductor are strongly affected by intercalation. During recent years, stage-1 iodine-intercalated  $\text{IBi}_2\text{Sr}_2\text{CaCu}_2\text{O}_8$  has been synthesized<sup>1-3</sup> and its crystal structure determined by high-resolution electron microscopy.<sup>4,5</sup>

Iodine has been found to intercalate between every set of Bi-O bilayers, leading to an expansion of their distance from 3.2 to 6.8 Å. These layers become virtually aligned and there is only one formula unit per unit cell for the idealized network (Fig. 1). The superstructure modulation remains nearly the same as in the parent material.<sup>6</sup> From various studies made so far on iodine-intercalated materials, the situation is not yet clear about the microstructure conversion from Bi 2:2:1:2 to  $\text{IBi}_2\text{Sr}_2\text{CaCu}_2\text{O}_8$  the actual species present in the intercalated iodine layers and the interaction forces between the iodine layer and the adjacent ones.

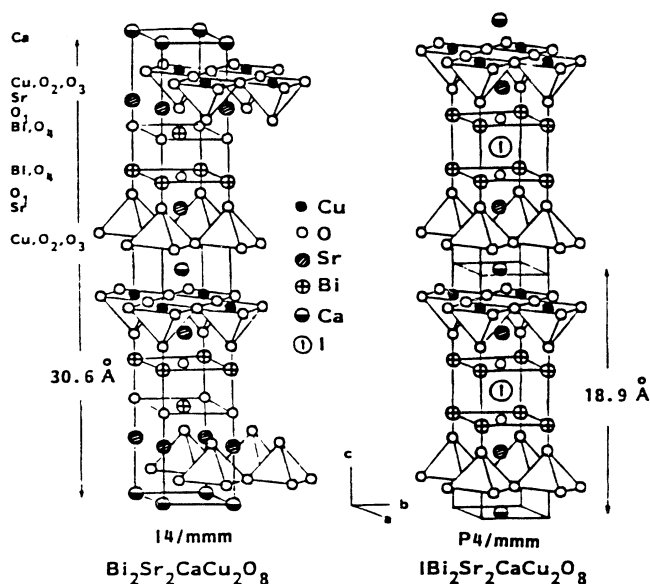


FIG. 1. Idealized spatial structures of  $\text{Bi}_2\text{Sr}_2\text{CaCu}_2\text{O}_8$  and  $\text{IBi}_2\text{Sr}_2\text{CaCu}_2\text{O}_8$ .

In this paper, we present our study on single crystals of  $\text{Bi}_2\text{Sr}_2\text{CaCu}_2\text{O}_8$  and stage-1 iodine-intercalated  $\text{IBi}_2\text{Sr}_2\text{CaCu}_2\text{O}_8$ . The materials will be characterized by resistivity measurements and by Raman microspectroscopy, the latter technique being known to be very helpful in the studies of superconductors and iodine species in charge-transfer interactions.<sup>6-11</sup>

The nature of the iodine species in the intercalated layers will be identified and the interaction forces between the iodine layers and Bi-O layers will be evaluated.

### II. EXPERIMENT

Single crystals of Bi 2:2:1:2 come from many sources.<sup>7,8,12</sup> They often contain Bi 2:2:2:3 and give two waves in resistivity and magnetic susceptibility measurements versus temperature. In such cases, their Raman spectra show two bands in the lower frequency range, at 60 and 51  $\text{cm}^{-1}$  which correspond to the Sr motion, respectively, in Bi 2:2:1:2 and Bi 2:2:2:3.<sup>13</sup> For this study, we select samples presenting only one phase. Nevertheless, these one-phase Bi 2:2:1:2 series have their  $T_c$  strongly dependent on the preparation parameters, especially on the oxygen pressure during the annealing stage.<sup>12</sup> We finally select monophase, untwinned single crystals with average sizes  $4 \times 2 \times 0.2$   $\text{mm}^3$  of Bi 2:2:1:2 for our experiment. These crystals will be revealed to have the highest  $T_c$  in the Bi 2:2:1:2 series and do not present Raman characteristics of Bi 2:2:2:3.<sup>13</sup>

Iodine-intercalated crystals of Bi 2:2:1:2 were then prepared by encapsulating iodine and Bi 2:2:1:2 crystals in a sealed silica tube under vacuum,  $10^{-3}$  Torr, and kept at a temperature of 170 °C for three days in a uniform temperature furnace, and then followed by a thermal gradient for condensing iodine in the lower temperature region of the tube.

The Raman spectra were recorded on a Dilor-Omars microspectrometer coupled with an optical microscope (spatial resolution of 1  $\mu\text{m}^2$ ) and an intensified 1024 channel photodiode array detector. The 514.5 and 457.9 nm lines from an ion argon laser Spectra Physics model 2016 and the 647.1 nm line of a krypton laser Spectra Physics model SP2000 were used as excitation sources. The Ra-

man spectra recorded in different areas across the thickness of a cleaved sample were identical, confirming the absence of any inhomogeneity in intercalation.

### III. RESULTS AND DISCUSSION

#### A. Raman spectrum of starting material Bi 2:2:1:2

From the result obtained by electron microprobe analysis (EMPA), the parent material Bi 2:2:1:2 has  $\text{Bi}_{1.87}\text{Sr}_{1.84}\text{Ca}_{1.00}\text{Cu}_{1.96}\text{O}_8$  composition, which is the average result from analyses of four different areas on a single crystal. The resistivity measurements give a rigorous single transition with zero resistivity  $T_c(R_0)$  at 97 K, the highest value obtained for a Bi 2:2:1:2 single crystal (Fig. 2).

The polarized Raman spectra of a Bi 2:2:1:2 single crystal are displayed in Fig. 3. A strong doublet centered at 653 and 627  $\text{cm}^{-1}$  is observed in the ZZ scattering symmetry. These two bands are found in all bismuth-based superconductors<sup>13</sup> presenting close, staggered, and identical Bi-O bonds along the  $c$  axis, in an idealized limiting structure  $I_4/mmm$ . They could correspond to the coupling of the stretching motions in these Bi-O bonds in the solid network. In Bi 2:2:1:2, this mechanical coupling is relatively weak, compared to that of the same nature in the Ti-O bonds of  $\text{Tl}_2\text{Ba}_2\text{CaCu}_2\text{O}_8$  (Ref. 7) and in the Cu-O bonds of  $\text{YBa}_2\text{Cu}_4\text{O}_8$ .<sup>9</sup> The higher frequency band, 653  $\text{cm}^{-1}$  for Bi 2:2:1:2, disappears each time one of the three conditions, close, staggered, or identical is missing.

For convenience we name this 650  $\text{cm}^{-1}$  frequency the staggered Bi-O motion.

The other Raman features of Bi 2:2:1:2 are located at 325, 287, 150, 117, and 60  $\text{cm}^{-1}$  which correspond to the in-phase oxygen motion in the Sr-O plane, the out-of-phase oxygen motion in the same plane, and the Cu, Bi, and Sr motions, respectively.<sup>14</sup> The latter is very sensitive to the mass effect in the adjacent layers induced by the number of calcium layers: it becomes 70  $\text{cm}^{-1}$  in Bi 2:2:0:1 and 51  $\text{cm}^{-1}$  in Bi 2:2:2:3.<sup>13</sup> The band at 460  $\text{cm}^{-1}$ , observed in XX and YY scattering geometries but absent in the ZZ spectrum, is assigned to  $B_1$  symmetry mode  $\text{Cu-O}_{2,3}$ .<sup>15</sup>

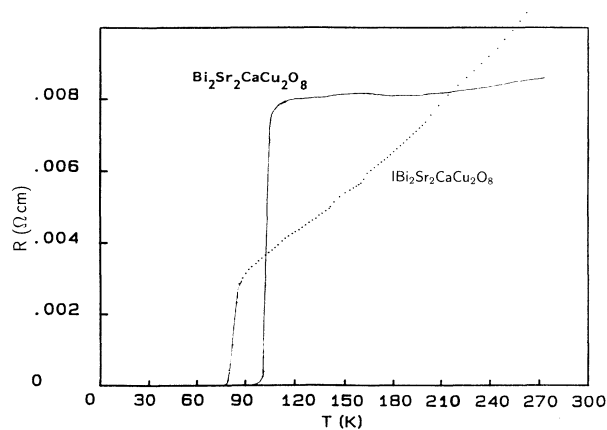


FIG. 2. Resistivity of  $\text{Bi}_2\text{Sr}_2\text{CaCu}_2\text{O}_8$  (—) and  $\text{IBi}_2\text{Sr}_2\text{CaCu}_2\text{O}_8$  (---) vs temperature.

#### B. Raman spectrum and microstructure of $\text{IBi}_2\text{Sr}_2\text{CaCu}_2\text{O}_8$

The iodine-intercalated  $\text{IBi}_2\text{Sr}_2\text{CaCu}_2\text{O}_8$  material prepared with the above method is no longer a single crystal throughout the whole thickness, but looks like a stacking of single-crystal lamellas. Its  $T_c$  becomes 78 K, lowered by 19 K compared to that of the parent crystal (Fig. 2). However, this decrease in  $T_c$  may not be due only to the iodine-intercalation effect, as we do not yet know if during the treatment some oxygen could have been removed from the material.

Anyhow, its Raman spectrum presents interesting changes. In particular, only one band at 621  $\text{cm}^{-1}$  could correspond to the Bi-O stretching motion along the  $c$  axis (Fig. 4). The collapse of two Bi-O bands into only one band could be correlated with the motion decoupling, as the Bi-O bonds become vertically aligned and very far apart in the idealized structure  $P4/mmm$  (Fig. 1).

This decoupling is similar to that observed when converting from Bi 2:2:1:2 to Bi 1:2:1:2, where structure  $P4/mmm$  also appears and where the single 627  $\text{cm}^{-1}$  band corresponds to the oxygen motion in aligned Bi-O-Bi bonds.<sup>16</sup>

Note that in Pb-doped Bi 2:2:1:2, the decoupling occurs as the antiparallel oscillators are no longer identi-

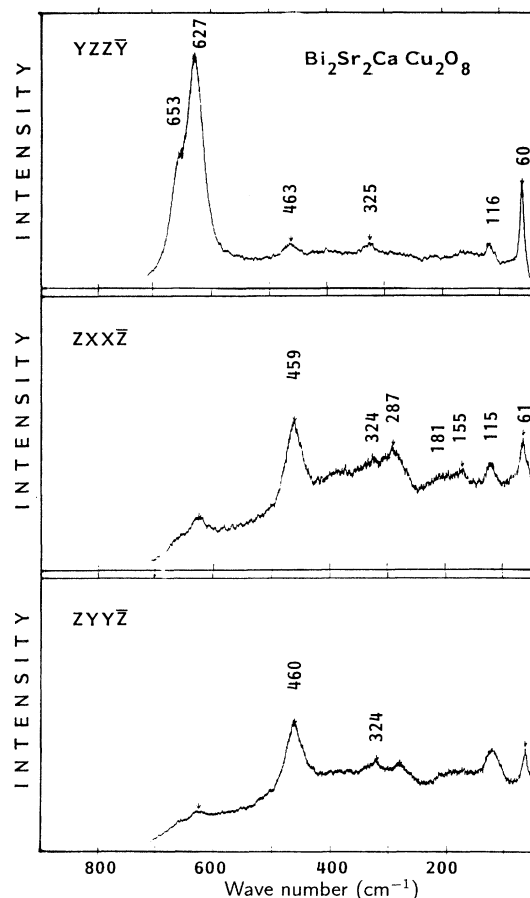


FIG. 3. Polarized Raman spectra of  $\text{Bi}_2\text{Sr}_2\text{CaCu}_2\text{O}_8$  single crystal.

cal.<sup>13,16</sup> In this case, the decoupling is also a proof that in lead doping, Pb takes the place of Bi.

With chloranil and tetrahydrofuran-doped Bi 2:2:1:2 we observe a similar collapse of the Bi-O stretching motions into only one band;<sup>17</sup> this could also correspond to the disappearance of the staggered configuration of the Bi-O planes and to the increase of their distance by intercalation.

Thus, the spectral and microstructure changes are mostly induced by steric intercalation and are much less dependent on the donor acceptor interactions, although these forces exist.

### C. Presence of unsymmetrical $I_3^-$ ions

Strong Raman bands are also observed at 149 and 107  $\text{cm}^{-1}$ . These bands are very strong compared to those known for the host component. Note, for instance, that the band at 461  $\text{cm}^{-1}$  in the  $XX$  spectrum, although still observable, is nearly drowned by the noise.

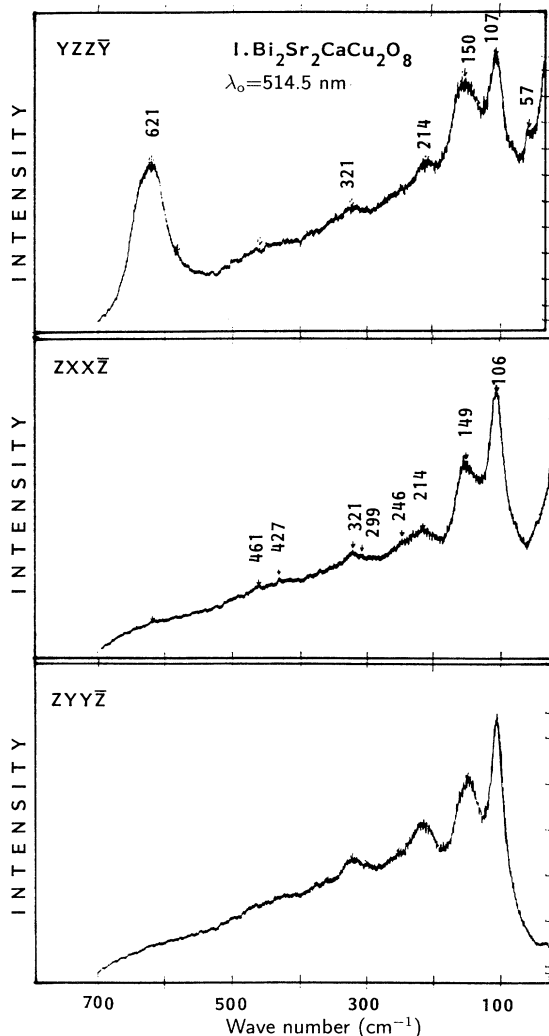


FIG. 4. Polarized Raman spectra of  $\text{IBi}_2\text{Sr}_2\text{CaCu}_2\text{O}_8$  single crystal.

The bands at 149 and 107  $\text{cm}^{-1}$  are quite distinct from the unique band usually observed for the  $I_2$  molecule<sup>18</sup> at 180–210  $\text{cm}^{-1}$ : thus, the presence of  $I_2$  must be ruled out. We assign them to unsymmetrical  $I_3^-$ . Remember that when  $I_3^-$  is linear with two unequal I-I bond lengths, its  $C_{\infty v}$  point group symmetry leads to  $\nu_1$  and  $\nu_3$  modes active in Raman scattering while in the linear symmetrical  $I_3^-$  ion, only  $\nu_1$  is Raman active.<sup>19</sup> As the  $\nu_3$  and  $\nu_1$  stretching modes of the unsymmetrical  $I_3^-$  ion generally occur within the same range,<sup>19</sup> our observed Raman features provide direct evidence of its presence. They cannot be associated with  $I_5^-$  or longer ions as their stretching motions are located at relatively higher frequencies.<sup>20</sup> Another fact against the presence of  $I_5^-$  is the lack of a resonance effect on its Raman spectrum when changing the excitation laser line from 514.5 to 457.9 nm, and then to 647.1 nm. In particular, with the latter excitation lying exactly at the absorption maximum of  $I_5^-$ , its resonance effect could be very strong, but experimentally this is not found to be the case.

On the contrary, strong support for the presence of  $I_3^-$  is its preresonance effect. This is because its absorption maxima are centered around 290 and 360 nm, giving the progression effectively observed for its fundamental  $\nu_1$  mode with overtones  $2\nu_1$ ,  $3\nu_1$ , and  $4\nu_1$  respectively at 107, 214, 321, and 427  $\text{cm}^{-1}$ . The antisymmetric  $\nu_3$  fundamental of asymmetrical  $I_3^-$  becomes Raman active at 149  $\text{cm}^{-1}$ , and the overtone  $2\nu_2$  at 299  $\text{cm}^{-1}$ , the latter is really detected although its intensity is weak.

We must mention that we cannot exclude the presence of  $I^+$  and  $I^-$  ions, as the monatomic species have no vibration in Raman scattering.

### D. Weak interaction between $I_3^-$ and adjacent layers

We also notice that the Bi-O stretching phonon decreases but only weakly from 627 to 621  $\text{cm}^{-1}$ . This small but reproducible shift indicates that the interaction between the  $I_3^-$  ion and the adjacent Bi-O layer exists but is relatively weak. As the Bi-O layers are believed to act as a charge reservoir for electrons which create holes in the Cu-O planes responsible for superconductivity, our results suggest that the major contribution to the change in  $T_c$  after iodine intercalation could be due mainly to suppression of the staggered configuration and the inter-layer expansion, and much less to the charge transfer between iodine and the adjacent layers, as this structure conversion is the main effect observed by iodine intercalation.

### E. Distribution of $I_3^-$ in the iodine layer

All the  $I_3^-$  Raman bands of  $\text{IBi}_2\text{Sr}_2\text{CaCu}_2\text{O}_8$  are broad. This band broadening suggests inhomogeneous distribution of  $I_3^-$  in the lattice with, of course, more than one iodine atom being off-centered, as the average I-I distance of 5.84 Å is longer compared to  $a = b = 5.4$  Å of the host cell.

The intensity of the  $\nu_1$  and  $\nu_3$  bands of  $I_3^-$  is relatively weaker in *ZZ* scattering geometry compared to *XX* and *YY* geometries, showing that the  $I_3^-$  ion is inclined in reference to the *ab* plane. This arrangement is consistent with the difference in the I-I-I distance and the *a* or *b* parameter.

#### ACKNOWLEDGMENTS

Support by the Indo-French Centre for the Promotion of Advanced Research is gratefully acknowledged. Laboratoire de Spectroscopie Moléculaire et Cristalline is Unité de Recherche Associée au CNRS No. 124.

\*Permanent address: North-Eastern Hill University, Shillong, India.

<sup>1</sup>X. D. Xiang, S. McKernan, W. A. Vanka, A. Zettl, J. L. Corkill, T. W. Barbee III, and M. L. Cohen, *Nature (London)* **348**, 145 (1990).

<sup>2</sup>X. D. Xiang, A. Zettl, W. A. Vaseka, J. L. Corkill, T. W. Barbee III, and M. L. Cohen, *Phys. Rev. B* **43**, 11 496 (1991).

<sup>3</sup>D. Pooke, K. Kishio, T. Raga, Y. Fukuda, N. Sanada, M. Nagashi, K. Kitazawa, and K. Yamafuji, *Physica C* **198**, 349 (1992).

<sup>4</sup>X. D. Xiang, W. A. Vaseka, A. Zettl, J. L. Corkill, M. L. Cohen, N. Kijima, and R. Gronsky, *Phys. Rev. Lett.* **68**, 530 (1992).

<sup>5</sup>N. Kijima, R. Gronsky, X. D. Xiang, W. A. Vaseka, J. Hou, A. Zettl, J. L. Corkill, and M. L. Cohen, *Physica C* **198**, 309 (1992).

<sup>6</sup>A. Yamamoto, M. Onoda, E. T. Muromachi, and F. Izumi, *Phys. Rev. B* **42**, 4220 (1990).

<sup>7</sup>P. V. Huong, A. L. Verma, J. P. Chaminade, L. Nganga, and J. C. Frison, *Mater. Sci. Eng. B* **5**, 255 (1990).

<sup>8</sup>K. H. Kim, P. V. Huong, E. Oh-Kim, M. Lahaye, S. K. Cho, and B. C. Kwak, *J. Less-Common Met.* **164**, 1193 (1990).

<sup>9</sup>P. V. Huong, J. P. Chaminade, J. C. Frison, Y. K. Park, J. C.

Park, K. H. Kim, and J. S. Park, in *High Temperature Superconductor Thin Films*, edited by L. Corra (Elsevier, Amsterdam, 1992), p. 125.

<sup>10</sup>P. V. Huong, *Physica C* **180**, 128 (1991).

<sup>11</sup>P. V. Huong, *J. Phys. (Paris) Colloq.* **52**, C 6, 151 (1991).

<sup>12</sup>I. Shigaki, K. Kitahama, K. Shibutani, S. Hayashi, R. Ogaria, Y. Kawate, T. Kawai, S. Kawai, M. Matsumoto, and J. Shirafuji, *Jpn. J. Appl. Phys.* **29**, L2013 (1990).

<sup>13</sup>P. V. Huong, A. L. Verma, R. Cavagnat, H. Kitahama, T. Kawai, M. Lahaye, and E. Marquestaut, *J. Alloys Comp.* **195**, 133 (1993).

<sup>14</sup>R. Liu, M. V. Klein, P. D. Han, and D. A. Payne, *Phys. Rev. B* **45**, 7392 (1992).

<sup>15</sup>M. N. Iliev and V. G. Hadjiev, *Physica C* **157**, 495 (1989).

<sup>16</sup>P. V. Huong, C. Lacour, and M. M'Hamdi, *J. Alloys Comp.* **195**, 691 (1993).

<sup>17</sup>P. V. Huong (unpublished).

<sup>18</sup>W. Kiefer and H. J. Bernstein, *Chem. Phys. Lett.* **26**, 5 (1972).

<sup>19</sup>E. M. Nour and L. Shahada, *Spectrochim. Acta Part A* **45**, 1033 (1989).

<sup>20</sup>E. M. Nour, L. H. Chen, and J. Laane, *J. Phys. Chem.* **90**, 2841 (1986).